

# DECENTRALIZED CARRIER PHASE ANGLE INTERPOLATION METHOD FOR 2D STRUCTURES

Nguyen Phu Cong<sup>1\*</sup>, Phan Quoc Dung<sup>2</sup>

<sup>1</sup>*Ho Chi Minh City University of Industry and Trade*

<sup>2</sup>*Ho Chi Minh City University of Technology, VNU*

\*Email: [congnp@huit.edu.vn](mailto:congnp@huit.edu.vn)

Received: 22 March 2023; Accepted: 8 May 2023

## ABSTRACT

Decentralized power converters coupled in series and parallel to cells (2D - 2 Dimensional) have been focused on research and application deployment. The method of implementing decentralized power converters is seen as a multi-level modulation technique. Implementation of this technique will allow dynamic modification of the system's structure when it is necessary to add or remove some cells; This is necessary in case of cell failure or optimization of a certain operating condition. This paper introduces the 2D structure and control technique according to the carrier pulse width modulation method (CPWM). Decentralized carrier phase angle interpolation (DCPAI) method for 2D structure, each cell in the 2D structure will communicate with neighboring cells to transmit and receive the necessary information for the phase shift carrier generation process. The carrier of each cell will be interpolated from the following information: position of cell in a row; position of cell in column; number of active rows and columns. Automatic carrier phase angle correction, proven parallel branch current balancing under normal start-up and dynamic reconfiguration are important issues. The proposed structure and control method are evaluated through simulation results on Matlab/Simulink software.

*Keywords:* Decentralized control, carrier phase shift, multilevel power converter, flying capacitor multilevel converter.

## 1. INTRODUCTION

The field of power electronics is always evolving, present in most industrial and commercial applications [1, 2]. Researchers have constantly searched for new structures, researched control algorithms to improve power quality [3, 4], improve harmonics, improve flexibility, and reliability in the control and operation [2, 5]. One of the issues of interest is multi-level power converters and control methods [6, 7]. The benefits that multi-level power converters bring is the complex calculation process of multi-objective problems: management, control, voltage balance between cells [8, 9]; manage, control and balance current between branches; common mode voltage regulation [10], etc. Besides, normally the number of levels of the output voltage will be proportional to the number of switches [11]. As the number of levels increases, processors must be able to connect and control many devices at the same time [12]. This is one of the difficulties when implementing multilevel technology in power converters.

A decentralized control technique to divide the tasks, roles and processing capabilities into local controllers has been researched and deployed in power converters [13, 14]. The decentralized power converter structure will consist of many small cells linked together.

Decentralized power converters in series with cells can the output voltage amplitude or adjust the output voltage level. This process can be quickly done by adding or removing some cells.

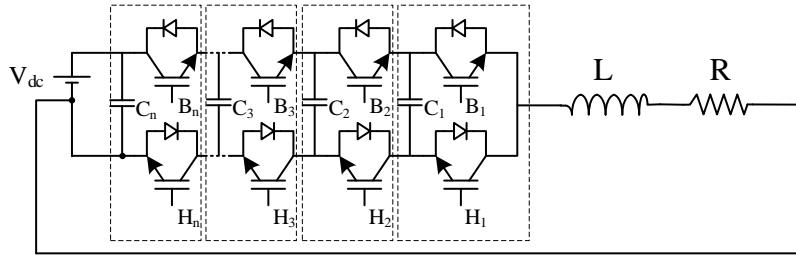


*Figure 1. Multicell in series DC/DC converter.*

The output voltage is the sum of the voltages of the active cells in the series loop. In addition, adding or removing several cells in parallel allows the appropriate current to be supplied to the load, which can flexibly meet different power needs. The combination of series-coupled and parallel-coupled cells allows the voltage and current response to be adjusted for other loads and power ranges, allowing the power converters to operate optimally.

In a conventional power converter, the central processor generates multi-carriers with appropriate carrier amplitudes, positions, and angles. When the system needs to be reconfigured, all settings and carriers must be recalculated. The process is sometimes not possible or takes a long time to re-establish. In the decentralized control architecture of power converters, each cell computes its carrier with the appropriate frequency, position and offset angle. The incoming wave is synthesized from the information received by the cell from neighboring cells. With cell-series structure, the information can be carrier amplitude [15], carrier phase angle [15–17], forward cell position, total number of active cells [15]. With a parallel cell structure, the necessary information can be the carrier phase angle [18], the position of the front cell, the total number of active cells [15].

Carrier pulse width modulation for 2D structures has been of interest and published by some scientists. With the structure of multiple cells coupled in series and parallel, research [19,20] shows that the cell carrier is synthesized from the communication process in rows and columns. Each cell in the structure has received position information from the previous cell in a row; transmits its own position to the next cell in the same row; transmits and receives phase angles of two neighboring cells to determine the total number of cells in the row. A similar algorithm and setup are done for the column. The connection and algorithm show that it is quite complicated, and the computational volume of each cell is relatively high.

This paper introduces a method to find the carrier phase angle of cells in parallel and series coupled multi-cell converter structures. The study uses the DC/DC converter structure as an example to illustrate the proposals. The proposed carrier phase angle interpolation method for each cell is based on the information and location of neighboring cells. The number of established communication is small, it is only a loop that retrieves position information, so the accuracy and reliability is very high, the carrier is interlaced strictly within 360 degrees. Proposals are verified through a decentralized power converter on Matlab Simulink software. The content of the verification includes issues: The arrangement of the carrier phase angle, the carrier interlacing, the ability to adjust the balance of the current between the branches, the voltage of the cells in the case of regular operation and when dynamic refactoring.

## 2. PROPOSED CARRIER PHASE ANGLE INTERPOLATION METHOD FOR 2D STRUCTURES

### 2.1. 2D structure and proposed carrier phase angle interpolation algorithm

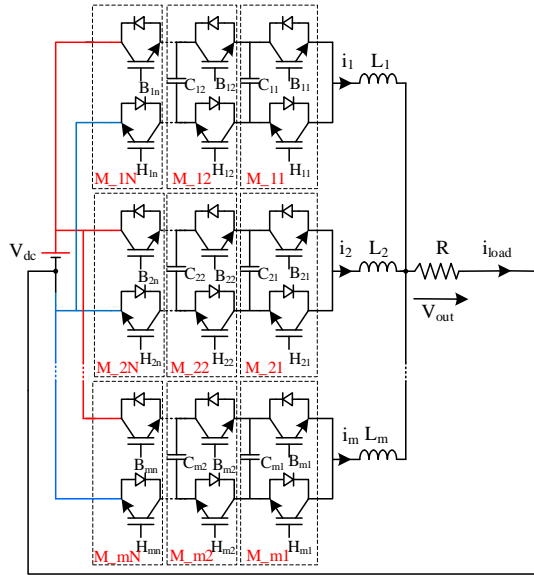


Figure 2. The IGBT connection of multicell in series/ parallels DC/DC converter



Figure 3. Decentralized control connection between cells with carrier phase angle interpolation algorithm for 2D structure

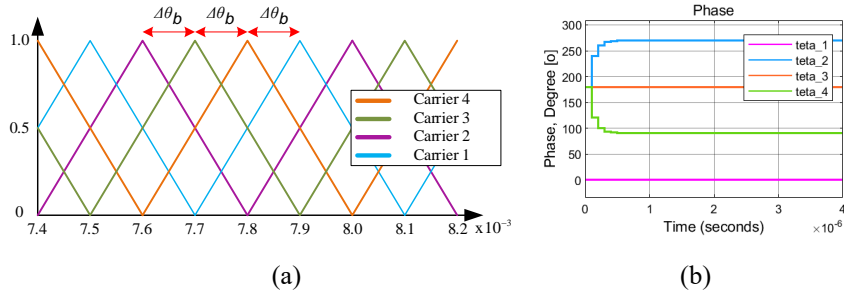


Figure 4. Phase angle and arrangement of phase shift carriers; a) phase shift carriers; (b) carrier phase angle

Table 1. Input/output functions of one cell

Symbol	Functions
Input	
$EN$	Enable/disable cell activity
$V_{rf} in$	Get reference voltage amplitude from master cell
$V_m in$	Get amplitude modulated voltage from front cell
$p_V in$	Get location information from cell $n-1$ in a row
$t_V in$	Get total number of cells from cell $n-1$ in a row
$t_H in$	Get total number of cells from cell $n-1$ in a column
$p_H in$	Get location information from cell $n-1$ in a column
$clk in$	Get synchronization pulse from master cell
$i_{m-1}$	Branch current $m-1$
$i_{m+1}$	Branch current $m+1$
$i_m$	Branch current $m$
Output	
$p_V out$	Transmit position to cell $n+1$ in a row
$t_V out$	Transmit the total number of cells to cell $n+1$ in a row
$p_H out$	Transmit position to cell $n+1$ in a column
$t_H out$	Transmit the total number of cells to cell $n+1$ in a column
$V_{rf} out$	Transfer the reference voltage to the next cell
$V_m out$	Transmits the modulated voltage to the next cell
$clk out$	Transmit the synchronous pulse to the next cell
$B$	PWM control signal $B$ of cell $n$
$H$	PWM control signal $H$ of cell $n$
Internal variable	
$\theta_n$	Carrier phase of cell $n$

This paper presents the decentralized control multi-phase, multi-level power converter using the serial and parallel structure of cells as shown in Figure 2 as the research object. Each cell consists of two components: a power circuit and a cell controller. The power circuit of each cell consists of two opposing impulse-controlled IGBTs and a binding capacitor. If the cell is connected to a DC voltage source, there is no associated capacitor. The controller of each cell has input and output signal pins shown in Table 1. The connection and information exchange between cells is done according to Figure 3.

The carrier pulse width modulation applied to the structure shown in Figure 2, 3 requires each control cell to synthesize for itself a high frequency carrier, amplitude from 0 to 1 and the phase angle must be such that so that the phase angle difference between 2 neighboring

cells does not change. A typical example for a 4-carrier arrangement is as shown in Figure 4a, where the phase angles of the four carriers are 90 degrees apart, as shown in Figure 4b. At the time of start-up, the phase angle of the carriers may start with a different value; After several loops, the carrier phase angle of each cell is uniformly corrected between 0 and 360 degrees.

In carrier aggregation, power converter used row-by-column and locating communication [19], using a communication loop using equation (1) to determine the number of cells in the rows and columns; calculate the required phase shift angle for cells in rows and columns. This shows that the number of communication needs to be established is relatively high and the calculation algorithm of the cells is relatively complex. This study presents an approach to determining the distributed carrier phase angle of cells in a system consisting of  $N_{t\_V}$  cells connected in series in the same row and  $N_{t\_H}$  in parallel rows. Information exchanged between cells includes only the position of the previous cell in the row and the total number of cells in a row; position of the previous cell in the column and the total number of cells in a column. The number and function of the signal pins of the cell are shown in Table 1. The algorithm for determining the carrier phase angle for each cell is implemented in the following sequence: Determining the position and total number of cells in a row is done with the ordinal numbering method, specifically by implementing equation (2). In rows, the positioning signal of the previous cell reaches the cell only. specified  $p_{V\_in}$  is added one and sent to the output of specified cell  $p_{V\_out}$ . Thus the value of the output  $p_{V\_out}$  is the position of the cell in a row. The value of the  $p_{V\_out}$  of the last cell in the main link chain is the total number of active cells in a row, this output is connected to the  $t_{H\_in}$  input of the first cell. This signal is transmitted to all cells in a row in turn as in equation (3). The process of determining the position and the total number of cells in the column is done similarly to equations (4)-(5) presented.

$$\begin{cases} \theta_n^{k+1} = \theta_n^k + K(\theta_n^{\sim k+1} - \theta_n^k), \text{ with } K \leq 0.66 \\ \theta_n^{\sim k+1} = \text{mod}(\theta_{n+1}^k + 0.5\text{mod}(\theta_{n-1}^k - \theta_{n+1}^k, 360), 360) \end{cases} \quad (1)$$

$$p_{V\_out}^k = p_{V\_in}^k + 1 \quad (2)$$

$$t_{V\_out}^k = t_{V\_in}^k \quad (3)$$

$$p_{H\_out}^k = p_{H\_in}^k + 1 \quad (4)$$

$$t_{H\_out}^k = t_{H\_in}^k \quad (5)$$

Where  $N_t$  is the total active cells in the system as shown in equation (6). Then the phase angle difference of 2 neighboring carriers is determined by expression (7).

$$N_t^k = t_{V\_out}^k * t_{H\_out}^k \quad (6)$$

$$\Delta\theta_b^k = \frac{360}{N_t} \quad (7)$$

Then the carrier phase angle of the cell is determined by equation (8)

$$\theta_n^k = \Delta\theta_b^k * [(p_{V\_out}^k - 1) * t_{H\_out}^k + (p_{H\_out}^k - 1)] \quad (8)$$

## 2.2. Decentralized control method of parallel branch current

One of the critical research problems of parallel branch configuration is to ensure that the branch currents are controlled and stable; then the branch currents share the capacity to power the load; branch currents satisfy the expression (9).

$$i_1 \approx i_2 \approx \dots \approx i_m \approx \frac{i_{Load}}{m} \quad (9)$$

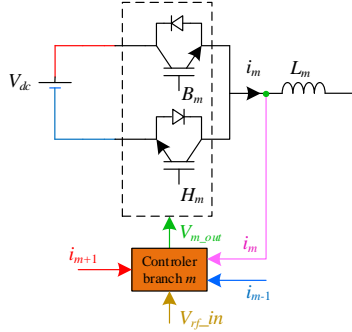


Figure 5. Current control diagram of branch

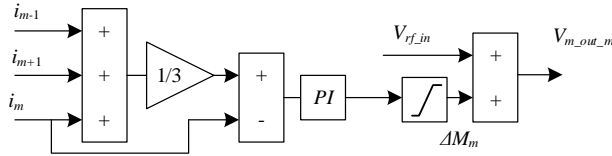


Figure 6. The process of executing the current control program of branch m

To achieve this relative balance, an algorithm is applied to balance the distributed currents between the branches of the power converter. Figure 5 shows a branch current control diagram  $m$ , in which the controller in each unit will receive its current information ( $i_m$ ), of two adjacent branches ( $i_{m-1}$ ,  $i_{m+1}$ ) and both reference modulation factor ( $V_{rf\_in}$ ). Recent research works have published several methods to balance the distributed currents between branches of DC/D power converters. The modules of each branch then receive feedback on the instantaneous currents of the branch itself and two neighboring branches. The branch current under consideration is compared with the average value of the three neighboring branches, this error produces a control signal  $PI$  correcting a quantity  $\Delta M_m$  into the reference signal  $V_{rf\_in}$  of the branch as shown in Figure 6. For DC/DC modulation technique, the quantity  $\Delta M_m$  affects the response of the output voltage to the desired voltage reference signal. The limiting step  $[-\beta \beta]$  is performed to ensure that the output voltage deviation is within the allowable limits. The control problem to accurately stabilize the output voltage on the load is considered by voltage closed-loop feedback control [17, 18, 21].

The cells in the power converter using the DCPAI method execute the program according to the algorithm diagram shown in Figure 7, the details are as follows:

Figure 7a: Signals required for cell carrier modulation include: input enable  $EN$  operation; input receive position and total number of cells from the previous cell in rows  $p_V\_in$ ,  $t_V\_in$ ; according to column  $p_H\_in$ ,  $t_H\_in$ , output transmits the part; and the total number of cells to the next cell according to the row  $p_V\_out$ ,  $t_V\_out$ ; according to the column  $p_H\_out$ ,  $t_H\_out$ ; the input receives the feedback current of the branch where the cell is located and the two neighboring branches  $i_m$ ,  $i_{m+1}$ ,  $i_{m-1}$

Figure 7b: If one cell has  $p_V\_in = 0$ , that cell belongs to column 1, cell will execute the program according to c, e, f, k. If  $p_V\_in = 1$  then that cell does not belong to column 1, cell will execute the program in terms of d, g, h, k.

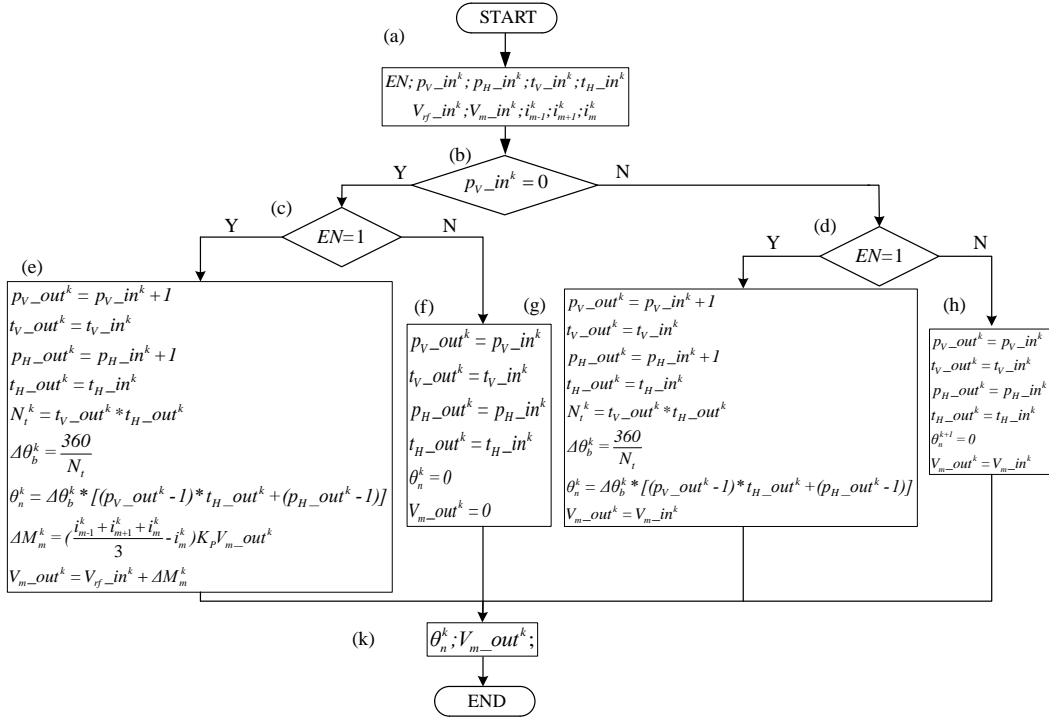


Figure 7. Algorithm flowchart of a cell for DCPAI method

Figure 7c: If a cell in column 1 is enabled  $EN=1$ , the algorithms in e) will be executed including: row and column positioning (2), (4); determine the total number of cells in rows and columns (3), (5); determine the total number of active cells in the; determine the fundamental phase difference angle of 2 neighboring carriers (7); determine the carrier phase angle of the cell (8); Receive current from 3 nearest branches and calculate modulation factor correction factor.

Figure 7f: When the cell in column 1 stops working, bypasses the cell's incoming and outgoing signals and the modulation voltage amplitude is set to zero, the phase angle and the carrier amplitude are set to zero.

Figure 7g: If one active cell is not in column 1, the algorithms that will be executed include: row and column positioning (2), (4); determine the total number of cells in rows and columns (2), (4); determine the total number of active cells in the system (6); determine the fundamental phase difference angle of 2 neighboring carriers (6); determine the carrier phase angle of the cell (8).

Figure 7h: If a cell is deactivated that is not in column 1, bypass the cell's incoming and outgoing signals and the modulation frequency and voltage amplitude is set to 0, and phase angle and carrier amplitude is assigned to 0.

Figure 7k: The signals needed for switching pulse modulation are carrier phase angle, and modulation voltage amplitude  $V_{m\_out}$ .

The structure and control method show that the cells in the system have an equivalent role. However, the system needs a cell to provide the synchronous clock, providing the reference signals, usually the first cell ( $C_{11}$ ) of the 2D power converter will be selected as the master cell. The reference voltage amplitude  $V_{rf}$  will be transmitted by the master cell to all cells in column 1 in turn. For the cells in column 1, the reference voltage amplitude is corrected to the modulation voltage  $V_m$  and transmitted through cells in the same row of that cell.

### 3. SIMULATION RESULTS AND DISCUSSION

#### 3.1. Configuration and simulation parameters

Without losing the generality of the proposed structure and control method, a power converter model as shown in Figure 2 is established including 6 parallel branches; each branch has 6 cells in series; the link between cells is established by capacitors of equal value; Simulation parameters are listed in Table 2. The simulation settings aim to:

Evaluate the ability to interleave the carrier phase angle of the cells in rows and columns, and the ability to interleave the carriers of all active cells in the system. This review simulation is conducted under normal operating conditions and dynamic reconstruction.

Evaluate the ability to adjust and balance the current between the branches of the DC/DC converter in the typical case and when removing or adding some branches.

Evaluate the ability to modulate the output voltage according to the reference voltage. In addition, the process also considers the effects of changing the reference voltage amplitude on the branch currents and output currents on the load.

Table 2. Simulation parameters

Parameter	Symbol	Unit	Value
Inductor	L	H	0.001
Link capacitors	C	$\mu\text{F}$	10
Resistor	R	$\Omega$	5
DC input voltage	$V_{dc}$	V	600
Switching frequency	$f_{sw}$	kHz	10
Sampling time	$T_s$	s	$10^{-6}$

#### 3.2. Simulation results

Figure 8 shows the process of setting the position of cells in rows and columns. For the 6-row and 6-column structure, the system needs 6 loops for the cell position to be stable, and 12 loops for determining the number of cells in the row and in the column. The interpolated carrier phase angle at each cell is calculated according to the row as shown in Figure 8a and column value as shown in Figure 8b, the total number of cells in the rows and columns, so the carrier phase angle will be stable after 12 loops as shown in Figure 9a, the carrier interlaced successfully as shown in Figure 9b. In general, with the proposed method, the number of iterations required for a successful configuration of the system is calculated according to equation (10) and the configuration time is calculated according to the equation (11). Where  $N_t$  is the max of  $N_{t_V}$  and  $N_{t_H}$ ,  $T_S$  is the sampling time.

$$N_{C\_DCPAI} = 2 * N_t \quad (10)$$

$$T_{C\_DCPAI} = N_{C\_DCPAI} * T_S \quad (11)$$

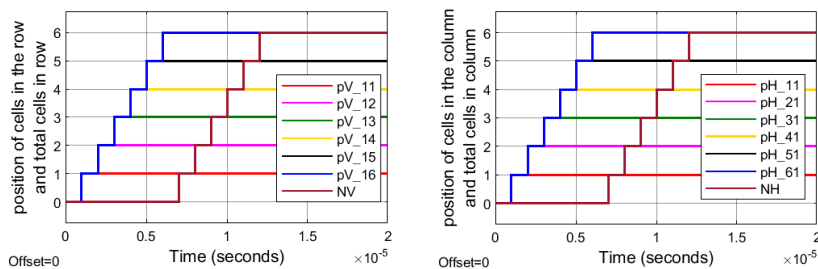


Figure 8. Position of cells in rows, columns and total cells in row, column

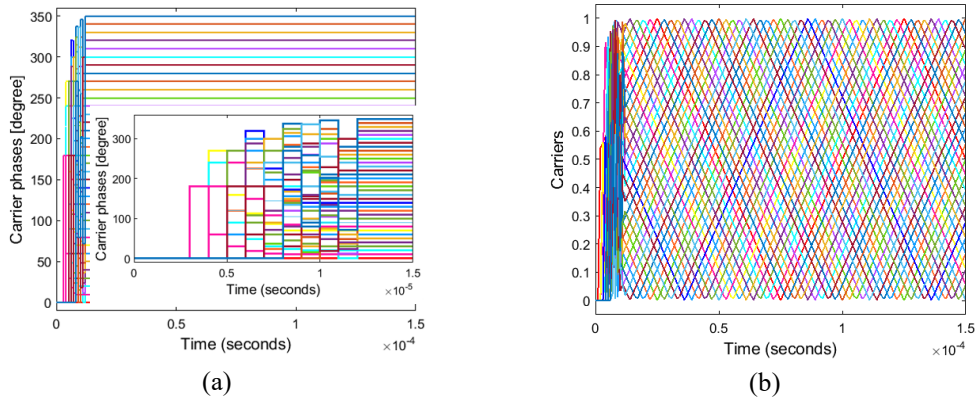


Figure 9. Carrier and carrier phase angles of a 6-row, 6-column structure; a) carrier phases; b) carriers.

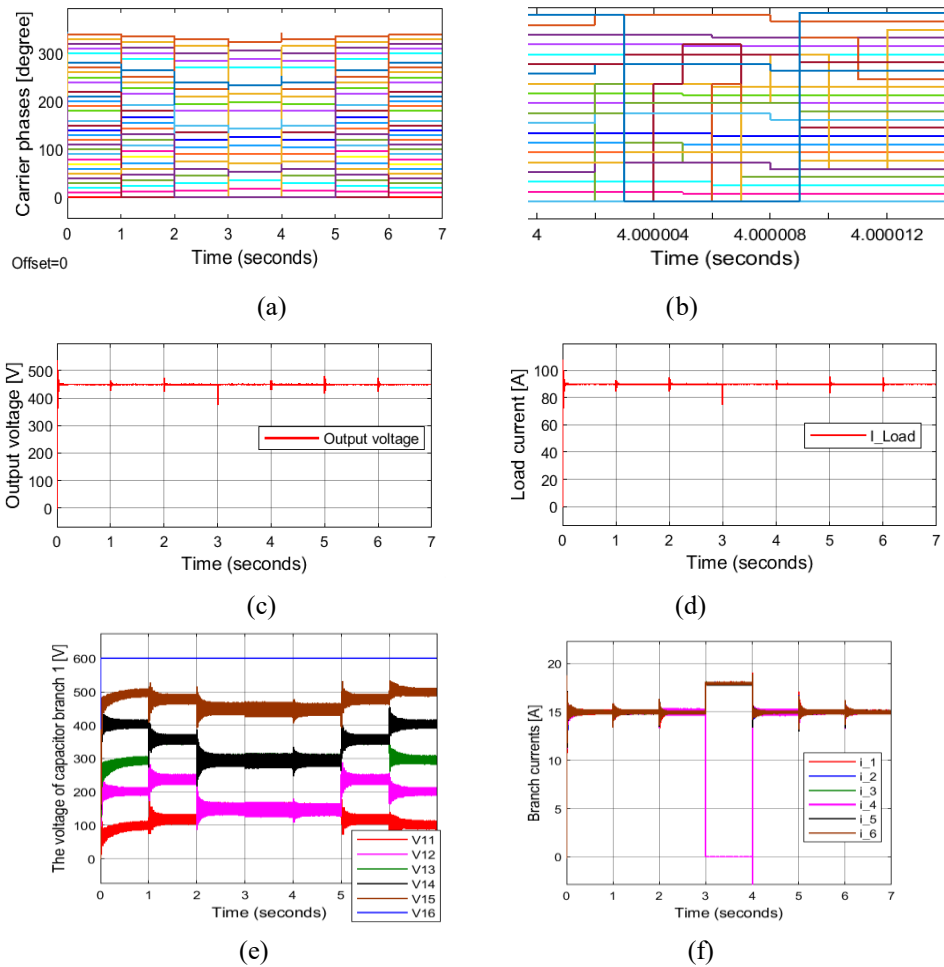


Figure 10. Configuration time of proposed method for 2D structure; modulation index is 0.75; a) carrier phases; b) zoom carrier phase angle at 0.4s; c) waveform output voltage; d) waveform load current; e) the voltage of capacitor branch 1; f) branch currents

Figures 10 show the response of carrier phase angle (Figures 10a), output voltage (Figures 10c), load current (Figures 10d), branch current (Figures 10e), and cell voltage of the 1st branch 2D structure (Figures 10f) when the system adjusts the number of rows and column. At 1 second, column 4 is stopped working, each row has 5 cells left, the carrier phase angle of

the cells is recalculated, ensuring  $\Delta\theta_b$  between 2 cells is 12 degrees, the voltage of each cell automatically dynamically reaches 120V, 240V, 360V, 480V and 600V values. The average current of the 6 branches is 15A. At 2 seconds, column 2 is removed, each row has 4 cells left, the carrier phase angle of the cells is reset to the new state,  $\Delta\theta_b$  between 2 cells is 15 degrees, the voltage of each cell is adjusted to 150V, 300V, 450V and 600V values. The average current of the branches is 15A. At the time of 3 seconds, the cells in row 4 stopped working, the system has 5 rows left, each row has 4 cells left, the carrier phase angle of the cells is adjusted, ensuring  $\Delta\theta_b$  between the 2 cells is 18 degrees, the voltage of each cell remains constant. Branch 4 current is 0A, the current of the remaining branches is quickly corrected to 18A. When row 4 is restored to operation at 4 seconds,  $\Delta\theta_b$  between the 2 cells is 15 degrees, the branch current 4 from 0 quickly adjusts to the value of 15A, the 6-branch current contributes 15A to the load. R has a current of 90A. The evaluation process is similar at 5s and 6s. The control process that changes the system structure shows that when an event occurs that changes the number of rows and columns, the system can be automatically adjusted; and switch to a new steady state to satisfy the requirement of the deflection angle of 2 adjacent carriers; The currents of the branches are shared equally.

#### 4. CONCLUSIONS

The simulation results demonstrate that the proposed algorithm, control topology and method have successfully interlaced the carrier phase angle of the activated modules in the 2D structure. The algorithm flowchart shows that the execution program of each module is quite simple, the connection number is minimal, the carrier phase angle is interpolated from the position and the total number of active modules ensures the program. The executor works with high reliability. The system configuration time depends on the number of modules present in the branches and the number of branches of the structure. The simulation results demonstrate the efficiency and can be fully met in the case of dynamic refactoring, thereby increasing flexibility in the control and operation of power converters. The study just stopped at the simulation results on Matlab/Simulink, it is necessary to have experimental studies to verify. The results will be conducted and announced in the experimental near future.

**Acknowledgements:** This work was funded by Ho Chi Minh City University of Industry and Trade (formerly Ho Chi Minh City University of Food Industry) (Contract number 138/HĐ-DCT dated October 1<sup>st</sup>, 2022).

#### REFERENCES

1. Wang Z., Wang Y., Chen, J., & Hu Y. - Decoupled vector space decomposition based space vector modulation for dual three-phase three-level motor drives. *IEEE Transactions on Power Electronics* **33** (2018) 10683-10697. <https://doi.org/10.1109/TPEL.2018.2811391>.
2. Sivasubramanian M., Boopathi C.S., Vidyasagar S., Kalyanasundaram V., Kaliyaperumal S. - Performance evaluation of seven level reduced switch anpc inverter in shunt active power filter with RBFNN-based harmonic current generation. *IEEE Access* **10** (2022) 21497–21508. <https://doi:10.1109/ACCESS.2021.3064715>.
3. Jacob J., Chitra A. - Field oriented control of space vector modulated multilevel inverter fed pmsm drive. *Energy Procedia* **117** (2017) 966-973. <https://doi:10.1016/j.egypro.2017.05.217>

4. Patkar F., Levi E., Jones M. - A six-phase multilevel space vector pwm algorithm for a dual-inverter supplied drive. 6<sup>th</sup> IET International Conference on Power Electronics, Machines and Drives **2012** (2012) 1-5. [https://doi: 10.1049/cp.2012.0245](https://doi:10.1049/cp.2012.0245).
5. Alyami S., Ali J.S.M., Almakhles D., Almutairi A., Obeidat M. - Seven level T-type switched capacitor inverter topology for PV applications. *IEEE Access* **9** (2021) 85049–85059. <https://doi:10.1109/ACCESS.2021.3084318>.
6. Roknuzzaman M., Yamaji T., Nakata H., Hamasaki S.I. - Power flow control using modular multilevel converter with circulating current control for 3-phase AC/AC conversion. 2020 23<sup>rd</sup> International Conference on Electrical Machines and Systems (ICEMS), Hamamatsu, Japan (2020) 597-602. <https://doi:10.23919/ICEMS50442.2020.9290877>.
7. Mora A., Urrutia M., Cardenas R., Angulo A., Espinoza M., Diaz M., Lezana P. - Model-predictive-control-based capacitor voltage balancing strategies for modular multilevel converters. *IEEE Transactions on Industrial Electronics* **66** (3) (2019) 2432-2443. <https://doi:10.1109/TIE.2018.2844842>.
8. Rahmati S., Veysinejad A., Bina M.T. - Capacitor ripple reduction with novel modulation scheme in modular multilevel converters. 2020 11th Power Electron. Drive Syst. Technol. Conf. **2020** (2020) 1-6. <https://doi:10.1109/PEDSTC49159.2020.9088441>.
9. Jafari M., Saadatmand S., Shojaeighadikolaei A., Jafarishiadeh F., Ghasemi A., Alshawish A.M., Ahmadi R. - New voltage balancing technique based on carrier-disposition pulse width modulation for modular multilevel converter. 2020 IEEE Power Energy Conf. Illinois **2020** (2020) 0-4. <https://doi:10.1109/PECI48348.2020.9064635>.
10. Robles E., Fernandez M., Zaragoza J., Aretxabaleta I., De Alegria I.M., Andreu J. - Common-mode voltage elimination in multilevel power inverter-based motor drive applications. *IEEE Access* **10** (2022) 2117-2139. <https://doi:10.1109/ACCESS.2021.3137892>.
11. Martinez-Rodrigo F., Ramirez D., Rey-Boue A.B., De Pablo S., Herrero-De Lucas L.C. - Modular multilevel converters: Control and applications. *Energies* **10** (11) (2017) 1-26. <https://doi.org/10.3390/en10111709>
12. Hu H., Yao W., Lu Z. - Design and implementation of three-level space vector PWM IP core for FPGAs. *IEEE Trans. Power Electron.* **22** (2007) 2234-2244. <https://doi:10.1109/TPEL.2007.909296>.
13. Xu B., Tu H., Du Y., Yu H., Liang H., Lukic, S. - A distributed control architecture for cascaded H-bridge converter with integrated battery energy storage. *IEEE Trans. Ind. Appl.* **57** (2021) 845–856. <https://doi:10.1109/TIA.2020.3039430>.
14. Xia B., Li Y., Li Z., Konstantinou G., Xu F., Gao F., Wang P. - Decentralized control method for modular multilevel converters. *IEEE Trans. Power Electron.* **34** (2019) 5117-5130. <https://doi:10.1109/TPEL.2018.2866258>.
15. Phan Q.D., Gateau G., Nguyen P.C., Cousineau M., To H.P., Nguyen B.A., Veit L., De Milly R., Hillesheim M.M. - A fast, decentralized, self-aligned carrier method for multicellular converters. *Appl. Sci.* **11** (2021) 1-34. <https://doi:10.3390/app11010137>.
16. Dung Phan Q., Nguyen P.C., To H.P., Nguyen B.A., Le Nguyen D.K., Nguyen Huu K.M., Pham L.N. - Decentralized capacitor voltage control of flying capacitor multilevel inverter. Proc. - 2021 Int. Symp. Electr. Electron. Eng. **2021** (2021) 238–243. <https://doi:10.1109/ISEE51682.2021.9418671>.
17. Gateau G., Dung P.Q., Cousineau M., Do P.U.T., Le H.N. - Digital implementation of decentralized control for multilevel converter. Proc. - 2017 Int. Conf. Syst. Sci. Eng. **2017** (2017) 558–562. <https://doi:10.1109/ICSSE.2017.8030937>.
18. Gateau G., Cousineau M., Mannes-Hillesheim M., Dung P.Q. - Digital decentralized

- current control for parallel multiphase converter. Proc. IEEE Int. Conf. Ind. Technol. **2019** (2019) 1761–1766. <https://doi:10.1109/ICIT.2019.8755049>.
19. Phan Q.D., Gateau G., Nguyen M.T., Cousineau M. - 2D Decentralized interleaving principle for multicell serial-parallel converters. Proc. Int. Conf. Power Electron. Drive Syst. **2019** (2019). <https://doi:10.1109/PEDS44367.2019.8998840>.
20. Phan Q.D., Gateau G., Nguyen M.T., Cousineau M., Thi Ngoc, T.P. - Decentralized interleaving and current control for multicellular serial-parallel converters. 2019 International Symposium on Electrical and Electronics Engineering (ISEE), Ho Chi Minh City, Vietnam (2019) 1-6. <https://doi:10.1109/ISEE2.2019.8921361>.
21. Grégoire L.A., Cousineau M., Seleme S.I., Ladoux P. - Real-time simulation of interleaved converters with decentralized control. Renewable Energy and Power Quality Journal **14** (2) (2016) 268-273. <https://doi:10.24084/repqj14.287>.

## TÓM TẮT

### PHƯƠNG PHÁP NỘI SUY GÓC PHA SÓNG MANG PHÂN TÁN CHO CẤU TRÚC 2D

Nguyễn Phú Công<sup>1\*</sup>, Phan Quốc Dũng<sup>2</sup>

<sup>1</sup>*Trường Đại học Công Thương Thành phố Hồ Chí Minh*

<sup>2</sup>*Trường Đại học Bách Khoa TP.HCM*

\*Email: [congnp@huit.edu.vn](mailto:congnp@huit.edu.vn)

Các bộ biến đổi công suất phân tán được ghép nối tiếp và song song (2D- 2 Dimensional) các mô-đun đã được tập trung nghiên cứu và triển khai ứng dụng. Phương pháp triển khai các bộ biến đổi công suất phân tán được xem như một kỹ thuật điều chế đa bậc. Khai triển kỹ thuật này sẽ cho phép hiệu chỉnh động cấu trúc của hệ thống khi cần phải thêm hoặc loại bỏ một vài mô-đun; điều này cần thiết trong trường hợp mô-đun bị hỏng hoặc tối ưu hóa một điều kiện vận hành nào đó. Bài báo này giới thiệu cấu trúc 2D và kỹ thuật điều khiển theo phương pháp điều chế độ rộng xung sóng mang. Phương pháp nội suy góc pha sóng mang phi tập trung (DCPAI- Decentralized carrier phase angle interpolation) cho cấu trúc 2D, mỗi mô-đun trong cấu trúc 2D sẽ giao tiếp với các mô-đun lân cận nhằm truyền, nhận các thông tin cần thiết cho quá trình tạo sóng mang dịch pha. Sóng mang của mỗi mô-đun sẽ được nội suy từ các thông tin: vị trí của mô-đun trong hàng, vị trí của mô-đun trong cột, số lượng hàng và cột đang được kích hoạt. Khả năng tự động hiệu chỉnh góc pha sóng mang, khả năng cân bằng dòng điện của các nhánh song song được kiểm chứng trong điều kiện khởi động bình thường và tái cấu hình động là các vấn đề cần quan tâm. Cấu trúc đề xuất, phương pháp điều khiển được đánh giá thông qua kết quả mô phỏng trên phần mềm Matlab/Simulink.

*Từ khóa:* Điều khiển phân tán, dịch mức sóng mang, bộ biến đổi công suất đa bậc, bộ biến đổi công suất đa bậc liên kết tụ điện.